

An Adaptive Control Strategy for Low Voltage Ride through Capability Enhancement of Grid- Connected Photovoltaic Power Plants

M Mojesh

M.Tech Student

Department of EEE,

Malineni Lakshmaiah Engineering College,
Singarayakonda, Prakasam, A.P.

J. Siva Sai, M.Tech

Professor

Department of EEE,

Malineni Lakshmaiah Engineering College,
Singarayakonda, Prakasam, A.P.

ABSTRACT

This project presents a novel application of continuous mixed - norm (CMPN) algorithm-based adaptive control strategy with the purpose of enhancing the low voltage ride through (LVRT) capability of grid-connected photovoltaic (PV) power plants. The PV arrays are connected to the point of common coupling (PCC) through a DC-DC boost converter, a DC-link capacitor, a grid side inverter, and a three-phase step up transformer. The DC-DC converter is used for a maximum power point tracking operation based on the fractional open circuit voltage method. The grid-side inverter is utilized to control the DC-link voltage and terminal voltage at the PCC through a vector control scheme.

The CMPN algorithm-based adaptive proportional-integral (PI) controller is used to control the power electronic circuits due to its very fast convergence. The proposed algorithm updates the PI controller gains online without the need to fine tune or optimize. The effectiveness of the proposed control strategy is compared with that obtained using Taguchi approach based an optimal PI controller taking into account subjecting the system to symmetrical, unsymmetrical faults, and unsuccessful reclosing of circuit breakers due to the existence of permanent fault. The validity of adaptive control strategy is extensively verified by the simulation results, which are carried out using MATLAB/SIMULINK software. With the proposed adaptive-controlled PV power plants, the LVRT capability of such system can be improved.

INTRODUCTION

Photovoltaic (PV) system will be one of the most promising renewable energy systems in the near future. The costs of the installed PV systems are continuously decreasing worldwide because of falling component average selling prices. Based on the statistics of the PV power plants 2014 industry guide report, the global PV system installations reached 136.7 GW at the end of 2013 and the cumulative market growth reaches 36%. Several factors affect the high penetration of the PV systems into electricity networks, such as environmental concerns, clean energy, increase in fuel price, political issues, and PV system cost reduction. In addition, installations of the MW PV power plants take only a few months. Large scale PV power plants were connected to the electric grid in the last few years. Because of this large integration with the electric grid, many problems arise and need to solve like low voltage ride through (LVRT) capability enhancement of such systems. With the high level of penetration of the PV power plants in the electric grids, maintaining the grid stability and reliability represents a greater challenge to the network operators. Recently, the utilities have released medium voltage grid codes to the PV systems that impose on these systems to contribute to and have a role in the grid support during grid faults. To fulfill these grid codes, the PV system needs to satisfy the LVRT capability requirement and remains in the grid-connected mode immediately after a disturbance takes place. Several methods have been used to study, analyze, and improve the LVRT capability of the PV systems. In the LVRT capability of single phase grid-connected PV systems

was presented using an extensive control method, which depends on controlling both the real and reactive powers out of the PV system. The authors extended their research work to apply the same control technique to transformer less PV systems. In the impact of dynamic performance of the PV systems on short term voltage stability was introduced. A cascaded proportional-integral (PI) control scheme was proposed to control the grid-side inverter. Moreover, many studies have utilized the PI controller for LVRT improvement of grid-connected PV systems. However, in all these previous reported studies, the design of the PI controller is based on the trial and error method which depends on the designer experience. Despite robustness of the PI controller and its usage in different industrial applications, it suffers from the sensitivity to parameters variation and nonlinearity of dynamic systems. Recently, different optimization techniques were implemented to solve this problem. Although these optimization methods are very effective to deal with such nonlinear systems, they require complex computational procedures, long times, and significant efforts. This represents a principle motivation of the author to apply the continuous mixed -norm (CMPN) algorithm- based adaptive PI controller to enhance the LVRT capability of grid-connected PV power plants. The CMPN algorithm is one of the newest adaptive filtering algorithms.

Adaptive filtering algorithms have been used to solve several engineering problems in different applications such as signal processing, electronics engineering, audio, speech, and language applications. Recently, these algorithms were explored in electric power systems, since affine projection algorithm was utilized to adapt the PI controller parameters in a wind energy conversion system. In these algorithms, a compromise should be taken into consideration between the algorithm complexity and the convergence speed. Many comparisons have been made among the proposed CMPN algorithm and other adaptive filtering algorithms.

The outcomes have demonstrated the high merging pace of the CMPN calculation over these calculations for various applications. In this venture, a novel utilization

of the CMPN calculation based versatile control methodology is exhibited for improving the LVRT ability of lattice associated PV control plants. The DC-DC help converter is utilized for a greatest power point following operation in view of the partial open circuit voltage strategy. The network side inverter is used to control the DC-connect voltage and terminal voltage at the point of common coupling (PCC) through a vector control plot. The CMPN calculation based versatile PI controller is utilized to control the power electronic circuits because of its quick joining. The proposed calculation refreshes the PI controller increases online with no compelling reason to calibrate or improvement.

The PV control plant is associated with the IEEE 39-transport New England test framework. The viability of the proposed control methodology is contrasted and that acquired utilizing Taguchi approach-based an ideal PI controller considering subjecting the framework to symmetrical, unsymmetrical issues, and unsuccessful reclosing of circuit breakers because of the presence of changeless blame. The legitimacy of the versatile control system is broadly confirmed by the reproduction comes about, which are completed utilizing matlab/simulink programming. To the best of the creator learning, the proposed control procedure has not been so far specified in power system literatures.

SOLAR CELL

Solar cells are the necessary apparatus of photovoltaic panels. Most are produced using silicon despite the fact that different materials are additionally utilized. Sun based cells exploit the photoelectric impact: the capacity of a few semiconductors to change over electromagnetic radiation straightforwardly into electrical current. The charged particles produced by the occurrence radiation are isolated helpfully to make an electrical current by a proper plan of the structure of the sunlight based cell, as will be clarified in short beneath. A sunlight based cell is essentially a p-n intersection which is produced using two distinct layers of silicon doped with a little amount of debasement iotas: on account of the n-layer, particles with one more valence electron, called benefactors, and on account of the p-layer, with one less valence electron,

known as acceptors. At the point when the two layers are consolidated, close to the interface the free electrons of the n-layer are diffused in the p-side, deserting a territory emphatically charged by the contributors. Likewise, the free openings in the p-layer are diffused in the n-side, abandoning a district adversely charged by the acceptors. This makes an electrical field between the two sides that is a potential hindrance to additionally stream. The harmony is come to in the intersection when the electrons and gaps can't outperform that potential obstruction and thus they can't move. This electric field pulls the electrons and openings in inverse ways so the current can stream in one way no one but: electrons can move from the p-side to the n-side and the gaps the other way. A chart of the p-n intersection demonstrating the impact of the specified electric field is represented in Figure1.

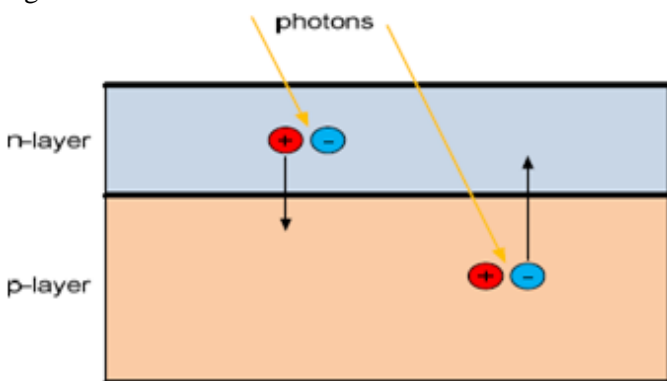


Figure 2.1 - Solar cell.

Equivalent circuit of a solar cell

The solar cell can be represented by the electrical model shown in Figure 2. Its current voltage characteristic is expressed by the following equation (1):

$$I = I_L - I_0 \left(e^{\frac{q(V-IR_S)}{AKT}} - 1 \right) - \frac{V - IR_S}{R_{SH}} \tag{1}$$

Where I and V are the sunlight based cell yield current and voltage individually, I₀ is the dim immersion current, q is the charge of an electron, A_n is the diode quality (ideality) factor, k is the Boltzmann steady, T is the supreme temperature and R_S and R_{SH} are the arrangement and shunt resistances of the sun powered cell. R_S is the resistance offered by the contacts and the mass semiconductor material of the sun oriented cell.

The cause of the shunt resistance R_{SH} is harder to clarify. It is identified with the non perfect nature of the p-n intersection and the nearness of polluting influences close to the edges of the cell that give a short out way around the intersection. In a perfect case R_S would be zero and R_{SH} unbounded. Nonetheless, this perfect situation is impractical and makers attempt to limit the impact of the two resistances to enhance their items.

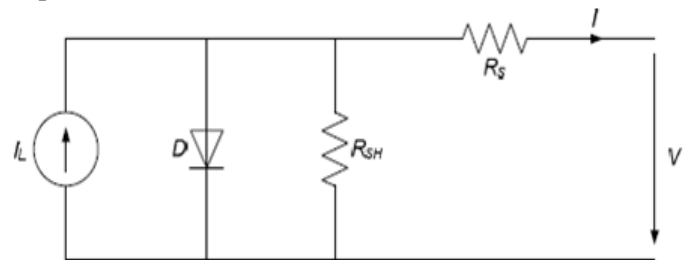


Figure 2.2 - Equivalent circuit of a solar cell.

Here and there, to streamline the model, as in the impact of the shunt resistance is not considered, i.e. R_{SH} is vast, so the last term in (1) is ignored. A PV board is made out of numerous sunlight based cells, which are associated in arrangement and parallel so the yield current and voltage of the PV board are sufficiently high to the prerequisites of the network or hardware. Considering the improvement specified over, the yield current-voltage normal for a PV board is communicated by condition (2), where n_p and n_s are the quantity of sun oriented cells in parallel and arrangement separately.

$$I \approx n_p I_L - n_p I_0 \left(e^{\frac{q(V-IR_S)}{AKTn_s}} - 1 \right) \tag{2}$$

Open circuit voltage, short circuit current and maximum power point

Two important points of the current-voltage characteristic must be pointed out: the open circuit voltage VOC and the short circuit current ISC. At both points the power generated is zero. VOC can be approximated from (1) when the output current of the cell is zero, i.e. I=0 and the shunt resistance R_{SH} is neglected. It is represented by equation (3). The short circuit current ISC is the current at V = 0 and is approximately equal to the light generated current I_L as shown in equation (4).

$$V_{oc} \approx \frac{AkT}{q} \ln \left(\frac{I_L}{I_0} + 1 \right) \quad (3)$$

$$I_{sc} \approx I_L \quad (4)$$

The maximum power is generated by the solar cell at a point of the current-voltage characteristic where the product VI is maximum. This point is known as the MPP and is unique, as can be seen in Figure 3, where the previous points are represented.

Types of solar cells

Over the past decades, silicon has been almost the only material used for manufacturing solar cells. Although other materials and techniques have been developed, silicon is used in more than the 80% of the production.

Silicon is so popular because it is one of the most abundant materials in the Earth's crust, in the form of silicon dioxide, and it is not toxic. Mono crystalline and polycrystalline silicon solar cells are the two major types of silicon solar cells. There is a third type, amorphous silicon, but the efficiency is worse than with the previous types so it is less used. Other new solar cells are made of copper indium gallium (di)selenite (CIGS) or cadmium telluride (CdTe). Much research and development (R&D) effort is being made to develop new materials, but nowadays there are no commercial substitutes to the above types of solar cells. In this section these different solar cells are reviewed. One of the most important characteristics of solar cells is the efficiency, which is the percentage of solar radiation that is transformed into electricity. It is measured under Standard Test Conditions (STC), irradiance of 1000 W/m², air mass coefficient (it characterizes the solar spectrum after the solar radiation has travelled through the atmosphere) A.M 1.5, and a cell junction temperature of 25°C. The higher efficiency, the smaller surface is needed for a given power.

This is important because in some applications the space is limited and other costs and parameters of the installation depend on the installed PV surface.

Mono crystalline silicon

Mono crystalline silicon solar cells are the most efficient ones. They are made from wafers (very thin slices) of single crystals obtained from pure molten silicon. These single crystal wafers have uniform and predictable properties as the structure of the crystal is highly ordered. However the manufacturing process must be really careful and occurs at high temperatures, which is expensive. The efficiency of these cells is around 15-18% and the surface needed to get 1 kW in STC is about 7 m².

Polycrystalline silicon

These cells are also made from wafers of pure molten silicon. However, the crystal structure is random: as the silicon cools, it crystallizes simultaneously in many different points producing an irregular structure: crystals of random sizes, shapes and orientation.

Amorphous and thin-film silicon

Amorphous silicon is the non-crystalline form of the silicon and it can be deposited as thin-films onto different substrates. The deposition can be made at low temperatures. The manufacturing process is simpler, easier and cheaper than in the crystalline cells. The weak point of these cells is their lower efficiency, around 6-8%.

Photovoltaic modules

PV modules are made from solar cells connected in series and parallel to obtain the desired current and voltage levels. Solar cells are encapsulated as they have to be weatherproofed and electric connections also have to be robust and corrosion free. The typical construction of a PV module can be seen in Figure 6.

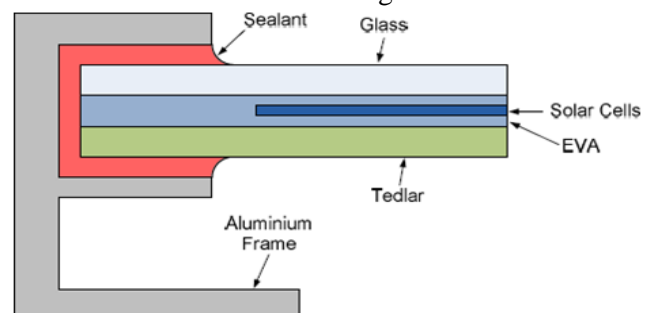


Figure 2.6 - PV Module typical construction.

As the cells are brittle, they are encapsulated in an airtight layer of ethylene vinyl acetate (EVA), a polymer, so the cells are cushioned and in that way are protected during transport and handling. The top cover is a tempered glass treated with an antireflection coating so the maximum light is transmitted to the cell. The underneath is a sheet of polyvinyl fluoride (PVF), also known as Tedlar, a synthetic polymer $(CH_2CHF)_n$ that constitutes a barrier to moisture and prevents the cell from chemical attack. An aluminium frame is used to simplify mounting and handling and to give extra protection. Frameless modules are sometimes used in facades for aesthetic reasons. This typical construction is used because the PV module has to “survive” outdoors for at least 20-25 years under different weather conditions, sometimes extreme. This construction assures at least the lifetime of the PV modules. In fact, PV panel manufacturers provide a guarantee of at least 20 years, for example BP Solar assures 85 % of minimum warranted power output after 25 years of service, 93 % of the minimum warranted power output at 12 years and a five-year warranty of materials and workmanship. Such a long guarantee is extremely long compared to most products and is due to the exceptional construction of PV modules.

LVRT

Grid dependability and security of supply are two imperative perspectives for vitality supply. Keeping in mind the end goal to maintain a strategic distance from control blackouts it is essential that power producing plants ought to have control capacities and assurance components. Before, these necessities were primarily satisfied by traditional power plants. Meanwhile, in any case, the offer of sustainable power sources in the aggregate power era has turned out to be significant to the point that these sources excessively should contribute, making it impossible to the lattice soundness.

In this way the transmission framework administrators have built up purported lattice codes with certain basic esteems and control qualities that the producing plants need to satisfy. An essential piece of these prerequisites is the purported LVRT capacity of creating plants. Be

that as it may, what precisely does this term mean? LVRT is short for Low Voltage Ride-Through (LVRT) and portrays the prerequisite that creating plants must keep on operating through brief times of low matrix voltage and not separate from the network. Here and now voltage plunges may happen, for instance, when extensive burdens are associated with the matrix or because of lattice shortcomings like lightning strikes or short circuits. Before, inexhaustible producing plants, for example, wind turbines were permitted to separate from the network amid such a blame and attempt to reconnect after a specific timeframe.

Today, in light of the noteworthy offer of renewables, such a technique would be deadly. In the event that an excessive number of creating plants detach in the meantime the entire system could separate, a situation which is additionally called a "power outage". Consequently the LVRT prerequisite has been built up which is intended to ensure that the creating plants remain associated with the matrix. Also numerous matrix codes request that the network ought to be bolstered amid voltage drops. Producing plants can bolster the lattice by sustaining receptive current into the system thus raise the voltage. Instantly after blame leeway, the dynamic power yield must be expanded again to the an incentive preceding the event of the blame inside a predefined timeframe. These prerequisites which toward the starting just connected to wind turbines, now additionally must be satisfied by photovoltaic frameworks (PV) and most as of late, by combined heat and-power plants (CHP).

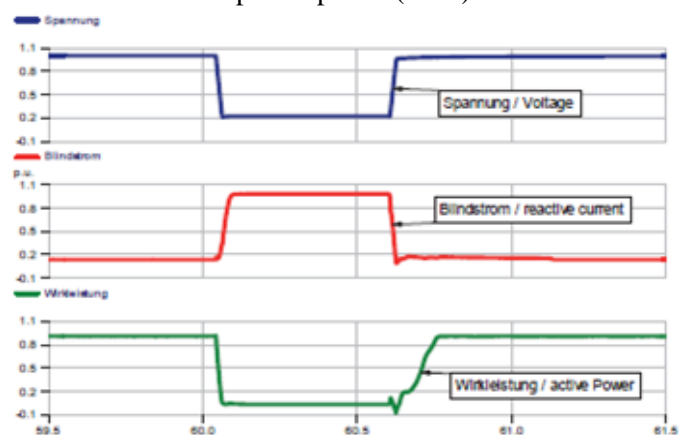


Fig. 3.1: Example of the results of a voltage drop test

SYSTEM MODELING

The PV arrays are connected to bus 18 of the test system through a DC-DC boost converter, a DC-link capacitor of 15 mF, a grid-side inverter, three-phase step up transformers, and double circuit transmission lines, as shown in Fig. 1(a). Fig. 1(b) illustrates a single line diagram of the IEEE 39-bus New England test system under study. This system is considered a compact version of the original New England System and it is used for realistic responses study. The IEEE 39-bus system includes 39 buses out of which 19 are load buses. There are 10 generators in the system. Bus 31 at which generator 2 is connected, is defined as the slack bus. The total load and generation of the system is 6098.1 and 6140.81 MW, respectively. The load model is considered to be constant current and constant admittance load. In order to test the PV power plant with the IEEE 39- bus system, the PV power plant is connected to bus 18. All data of the IEEE 39-bus system is available.

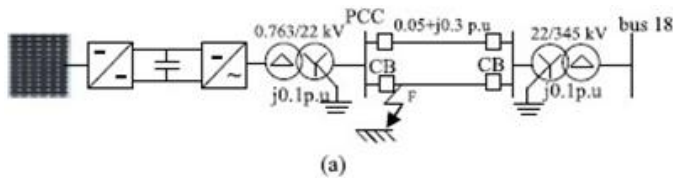


Fig. 4.1 Grid-connected PV power plant. (a) Connection of PV power plant

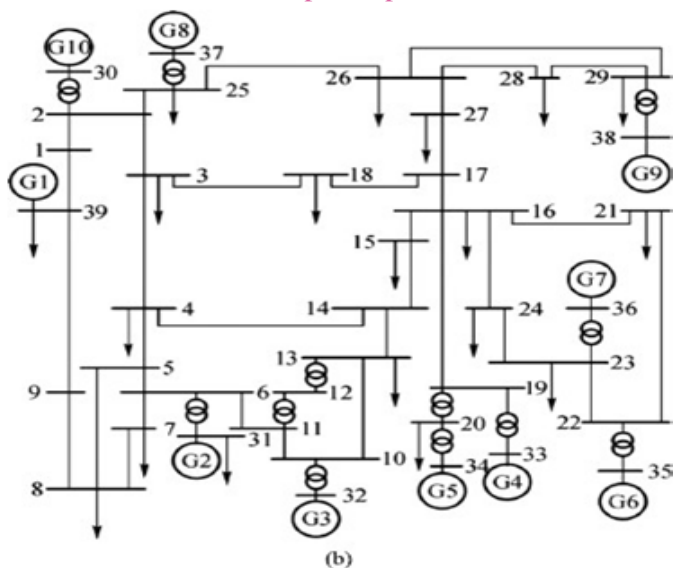


Fig. 1. Grid-connected PV power plant. (b) single line diagram of the IEEE 39-bus New England test system under study

CONTROL STRATEGY OF POWER ELECTRONIC CIRCUITS

A. DC-DC Boost Converter

A DC-DC boost converter is used to control the output voltage of the PV plant in order to satisfy the maximum output power condition. This is done by controlling the duty cycle of insulated gate bipolar transistor (IGBT) switch of the converter, as indicated in Fig. 2.

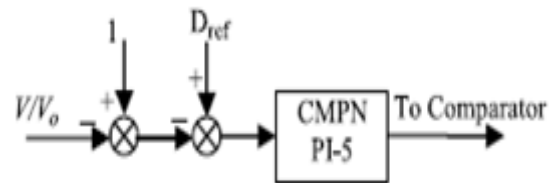


Fig. 4.2. Control of the DC-DC converter.

The duty cycle reference signal can be determined by the following equation:

$$D_{ref} = 1 - \frac{N_M K_M V_{oc-pilot}}{V_o}$$

An CMPN-based adaptive PI controller is used for this purpose. The controller output signal is compared with a triangular carrier waveform signal of 4-kHz frequency to generate the firing pulses of IGBT switch.

B. Grid-Side Inverter

A two-level, three-phase, six IGBT switches inverter is proposed in this study. The grid-side inverter is utilized to control the DC-link voltage and terminal voltage at the PCC through a vector control scheme, as illustrated in Fig. 3. The CMPN algorithm-based adaptive PI controllers are developed for this purpose. A phase locked loop (PLL) is dedicated to detect the transformation angle from the three- phase voltages at the PCC.

The output signals of the control scheme (Vq-ref and Vd-ref) are converted to three-phase sinusoidal reference signals , which are compared with a triangular carrier signal of 1-kHz frequency to produce the firing pulses of IGBT switches. The is maintained constant at 1.2 kV through the simulation using this pulse width modulation inverter.

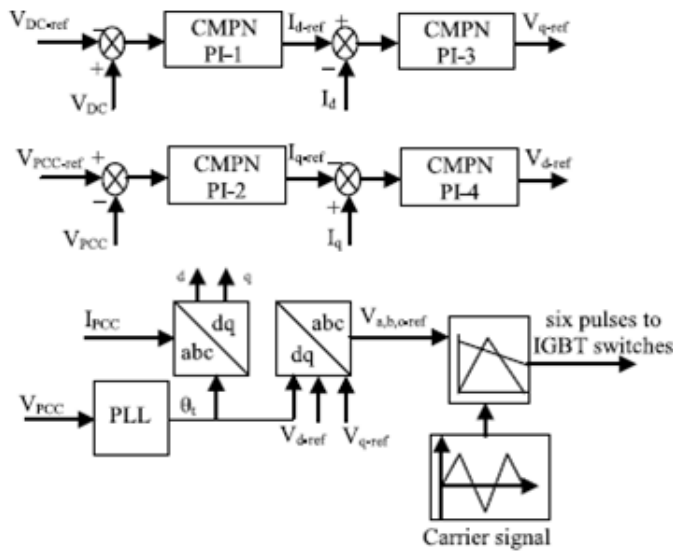


Fig. 4.3. Control block diagram of the grid-side inverter.

CMPN ADAPTIVE FILTERING ALGORITHM

One family of the adaptive filtering algorithms is the mixed- norm adaptive filters that have various forms. In the least mean mixed-norm (LMMN) adaptive filter was presented, where it combined the least mean square (LMS) and the least mean fourth (LMF) algorithms.

Moreover, a robust mixed-norm (RMN) algorithm was proposed and it combined the LMS algorithm with the least absolute deviation (LAD) algorithm. Then, a normalized RMN algorithm was introduced. The RMN algorithm depends mainly on the minimization of error norm and it can be expressed by the following equation:

$$J(k) = \lambda(k)E \{e^2(k)\} + (1 - \lambda(k)) E \{|e(k)|\}$$

Where $J(k)$ is the cost function that should be minimized, k is the iteration index, $\lambda(k)$ is a mixing parameter which adjusts the combination of error norms and it lies in the range of 0 and 1, and $e(k)$ is the output error of the adaptive filter that is defined as follows:

$$e(k) = d(k) - y(k)$$

$$y(k) = x^T(k)w(k)$$

Where $y(k)$ is the output vector of the adaptive filter, $x(k)$ is an input signals vector, $d(k)$ is the desired output signal vector, and $w(k)$ is the current weight vector of the adaptive filter. In the general concept of the λ -norm was presented to the LMS algorithm. However, this study concentrated on the standard LMS algorithm.

Recently, the λ -norm adaptive filtering algorithms were developed.

The CMPN algorithm can be defined as follows:

$$J(k) = \int_1^2 \lambda_k(p)E \{|e(k)|^p\} dp$$

Based on (10), the update of the weight vector of the CMPN adaptive filtering algorithm is written by the following formula:

$$w(k + 1) = w(k) - \mu \nabla_{w(k)} J(k)$$

In this study, all the adaptive PI controllers of the control strategies are based on the CMPN algorithm, which is used to adapt the proportional gain(k_p) and the integral gain(k_i) of the PI controllers. The online adaptation of the controller parameters is based. $X(k)$ represents the actual input signal to the summing point and $e(k)$ is the input signal of the PI controller. The update of the controller gains is expressed by the following formulas:

$$k_p(k + 1) = k_p(k) + \Delta k_p(k)$$

$$k_i(k + 1) = k_i(k) + \Delta k_i(k).$$

To guarantee the system stability, the initial values of the controllers' parameters are selected by using the black-box optimization technique which is a powerful simulation-based optimization implemented on matlab/simulink environment. Table I illustrates the initial values of the PI controllers' parameters. Then, the proposed adaptive algorithm can online update the controllers' parameters

SIMULATION RESULTS

Proposed system for 3LG temporary fault

The detailed model of a grid-connected PV power plant is presented. The model involves a complete switching model of the power electronic circuits with the proposed adaptive control strategy for obtaining realistic responses. The effectiveness of the proposed adaptive control strategy is compared with that obtained using Taguchi approach-based optimal PI controllers, taking into account subjecting the system to symmetrical, unsymmetrical faults, and unsuccessful reclosing of circuit breakers due to the existence of permanent fault as follows:

A. Successful Reclosure of Circuit Breakers (CBs)

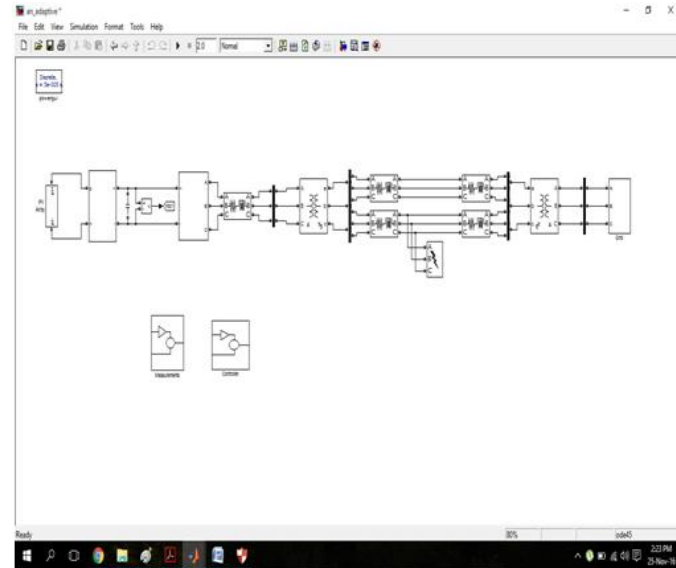


Fig:5.1- Simulation diagram of proposed system for 3LG temporary fault

Conventional system for 3LG temporary fault

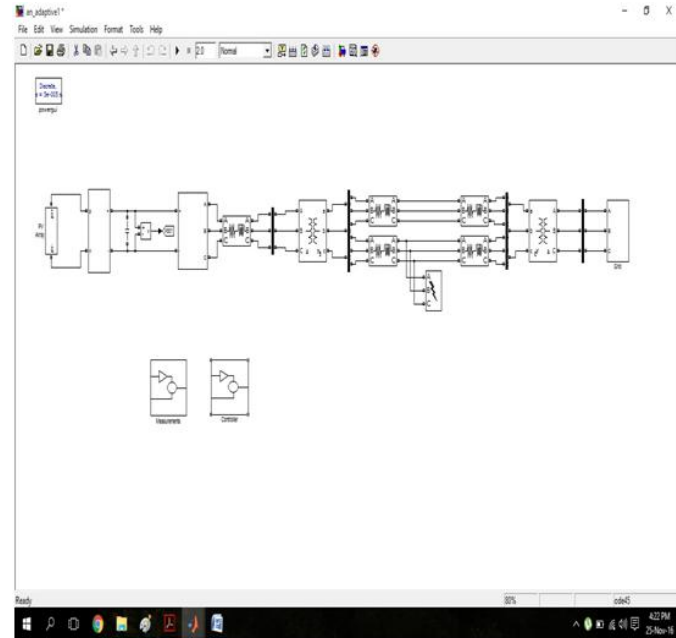


Fig:5.2-Simulation Diagram of conventional system for 3LG temporary fault

In this scenario, a three-line to ground (3LG) temporary fault takes place at time $t=0.1$ s with duration of 0.1 s at fault point F. The CBs on the faulted lines are opened at $t=0.2$ s to clear fault. Then, the CBs are reclosed again at

$t=1$ s. Successful reclosure of the CBs means reclosure under no fault condition.

Responses of proposed system for 3LG temporary fault

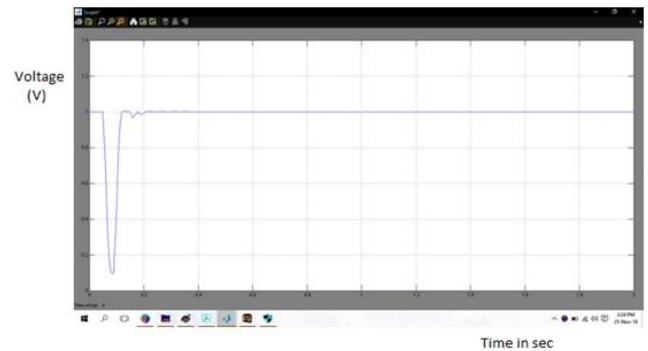


Fig:5.3(a) V_{pcc}

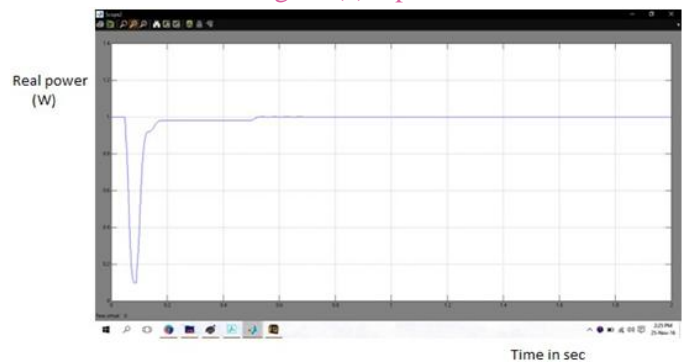


Fig: 5.3(b) Real power out of the PCC

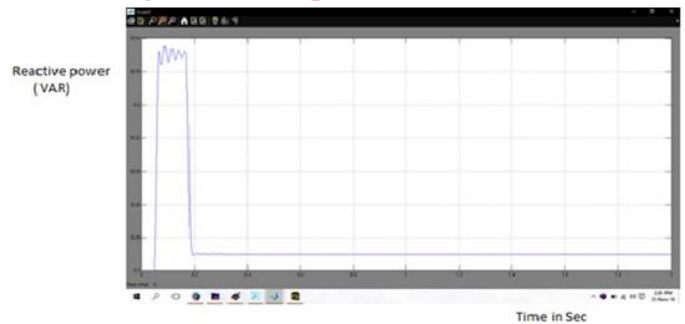


Fig:5.3(c) Reactive power out of the PCC

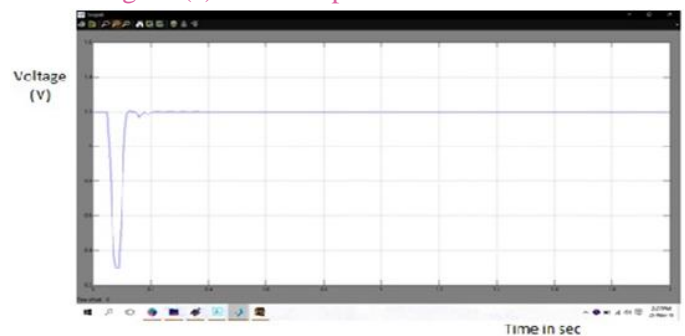


Fig:5.3(d) V_{dc}

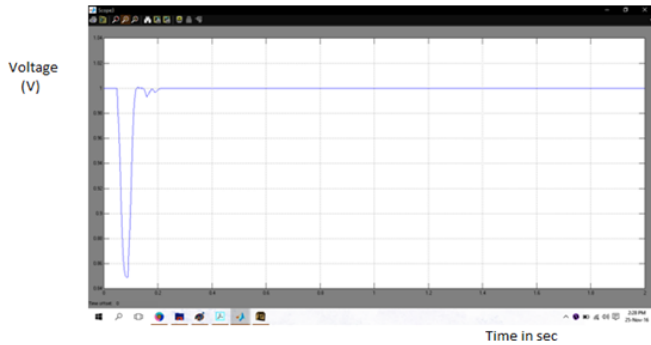


Fig:5.3(e) Voltage at bus 18

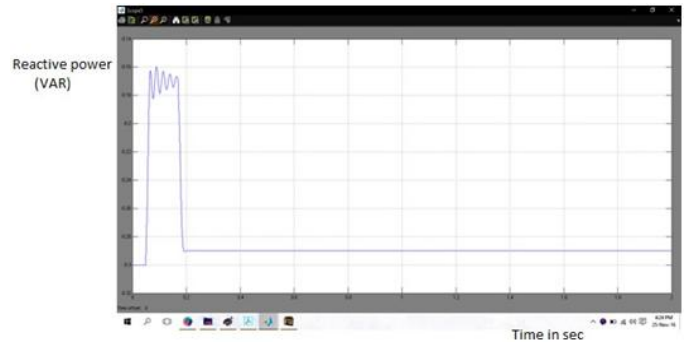


Fig:5.4(c) Reactive power out of the PCC

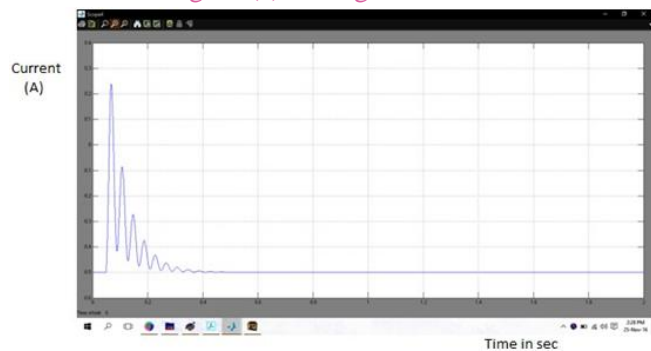


Fig:5.3(f) Inverter currents with the proposed controller
Fig. 5.3. Responses of proposed system for 3LG temporary fault.

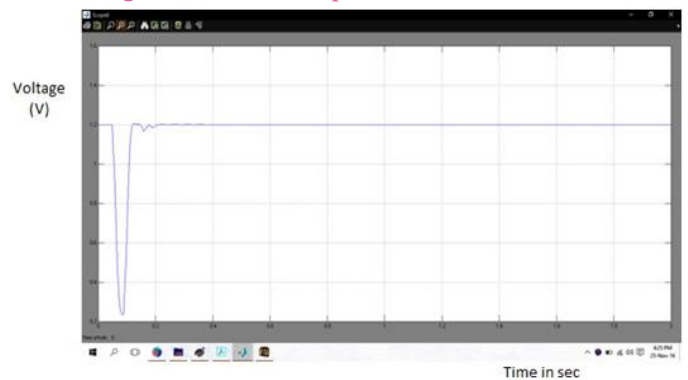


Fig:5.4(d) Vdc

Responses of conventional system for 3LG Temporary fault

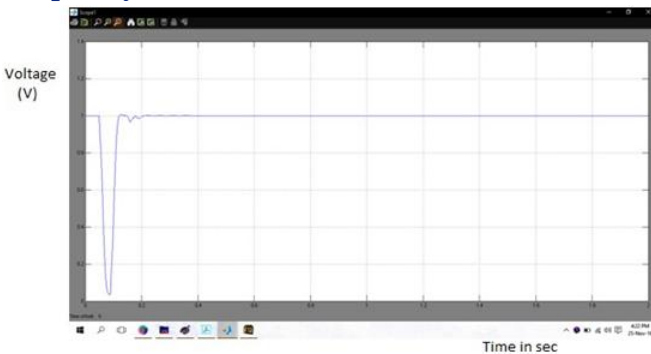


Fig:5.4(a) Vpcc

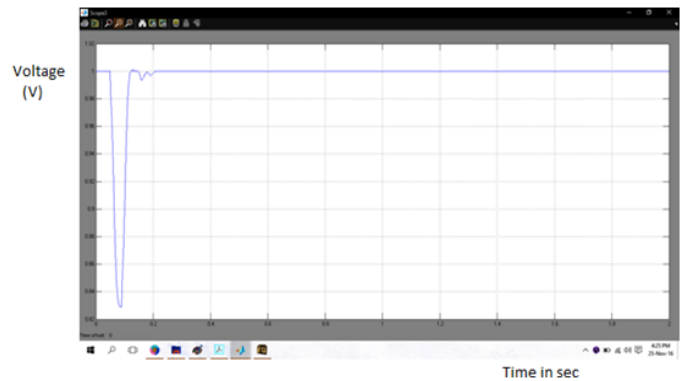


Fig:5.4(e) Voltage at bus 18

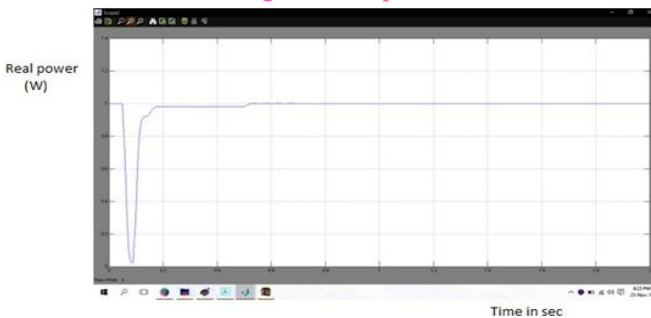


Fig:5.4(b) Real power out of the PCC

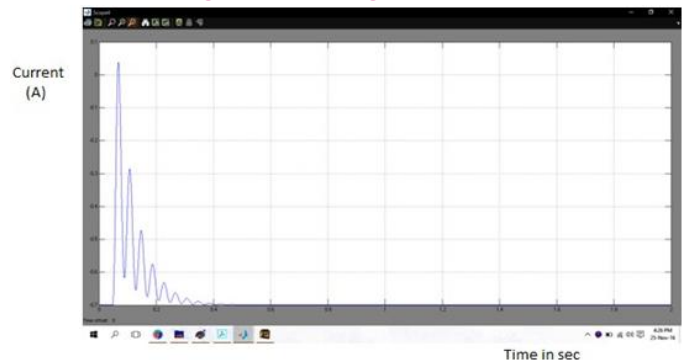


Fig:5.4(f) Inverter currents with the proposed controller
Fig. 5.4. Responses of conventional system for 3LG temporary fault.

The Vpcc drops immediately from the rated value (1 p.u) due to the effect of network disturbance and the grid side inverter delivers a good amount of reactive power that helps the Vpcc to return back to the rated value, as indicated in Fig. 3 & 4 (a). It is worth to note here that the Vpcc response using the CMPN-adaptive PI control strategy is better damped than that of using Taguchi approach-based an optimal PI control scheme, where it has lower maximum percentage undershoot, lower maximum percentage overshoot, lower settling time, and lower steady state error. Fig. 3 & 4 (b) points out the real power out of the PCC. It can be realized that the proposed controlled DC-DC converter controls efficiently the maximum output power of the PV plant at 1 p.u. The real power out of the PCC reaches final 0.96 p.u due to the converter, inverter, and transformer losses.

The reactive power out of the PCC, the Vdc, and voltage at bus 18 are shown in Fig. 3 & 4 (c)–(e), respectively. It can be noted that the responses using the proposed adaptive control strategy are very fast with minimum fluctuations. The online CMPN adaptive algorithm distinguishes a high speed convergence that updates the controller gains in an expedite way. Fig. 3 & 4 (f) indicates the direct axis and quadrature axis components of the inverter output currents (I_d and I_q).

It can be realized that the proposed controller limits the rms inverter currents during the network disturbance to a value of 1.2 p.u, which lies in an acceptable range.

CONCLUSION

This project has introduced a novel application of the CMPN algorithm-based adaptive PI control strategy for enhancing the LVRT capability of grid-connected PV power plants. The proposed control strategy was applied to the DC-DC boost converter for a maximum power point tracking operation and also to the grid-side inverter for controlling the Vpcc and Vdc. The CMPN adaptive filtering algorithm was used to update the proportional and integral gains of the PI controller online without the need to fine tune or optimize. The PV power plant was connected to the IEEE 39-bus New England test system. The simulation results have proven that the system

responses using the CMPN algorithm-based adaptive control strategy are faster, better damped, and superior to that obtained using Taguchi approach-based an optimal PI control scheme during the following cases:

- 1) subject the system to a symmetrical 3LG temporary fault;
- 2) subject the system to different unsymmetrical faults;
- 3) subject the system to a symmetrical 3LG permanent fault and unsuccessful reclosure of CBs.

It can be claimed from the simulation results that the LVRT capability of grid-connected PV power plants can be further enhanced using the proposed adaptive control strategy whatever under grid temporary or permanent fault condition. By this way, the PV power plants can contribute to the grid stability and reliability, which represents a greater challenge to the network operators. Moreover, the proposed algorithm can be also applied to other renewable energy systems for the same purpose.

FUTURE SCOPE

This project future work to be a novel application of the adaptive fuzzy algorithm-based neuro fuzzy control strategy for enhancing the LVRT capability of grid-connected PV power plants. The proposed control strategy was applied to the Dc-Dc boost converter for a maximum power point tracking operation and also the need to fine tune or optimize. And in the future realistic hardware to be implemented.

REFERENCES

- [1] PV Power Plants 2014 Industry Guide [Online]. Available: <http://www.pvresources.com>
- [2] D. L. Brooks and M. Patel, "Panel: Standards & interconnection requirements for wind and solar generation NERC integrating variable generation task force," in Proc. IEEE Power Eng. Soc. General Meeting 2011, Jul. 2011, pp. 1–3.
- [3] G. J. Kish, "Addressing future grid requirements for distributed energy resources," M.Sc. thesis, Dept. Elect. Comput. Eng., Univ. Toronto, Toronto, ON, Canada, 2011.



[4] Y. Yang, F. Blaabjerg, and Z. Zou, "Benchmarking of grid fault modes in single-phase grid-connected photovoltaic systems," *IEEE Trans. Ind. Applicat.*, vol. 49, no. 5, pp. 2167–2176, Sep./Oct. 2013.

[5] Y. Yang, F. Blaabjerg, and H. Wang, "Low-voltage ride-through of single-phase transformerless photovoltaic inverters," *IEEE Trans. Ind. Applicat.*, vol. 50, no. 3, pp. 1942–1952, May/Jun. 2014.

[6] K. Kawabe and K. Tanaka, "Impact of dynamic behavior of photovoltaic power generation systems on short-term voltage stability," *IEEE Trans. Power Syst.*, vol. 30, no. 6, pp. 3416–3424, Nov. 2015.

[7] M. S. El Moursi, W. Xiao, and J. L. Kirtley, "Fault ride through capability for grid interfacing large scale PV power plants," *IET Gener., Transm., Distrib.*, vol. 7, no. 5, pp. 1027–1036, 2013.

[8] Y. Wu, C.-H. Chang, Y. Chen, C. Liu, and Y. Chang, "A current control strategy for three-phase PV power system with low-voltage ride-through," in *Proc. IET Int. Conf. Advances on Power System Control, Operation, Management (APSCOM)*, 2012, pp. 1–6.

[9] M. K. Hossain and M. H. Ali, "Low voltage ride through capability enhancement of grid connected PV system by SDBR," in *Proc. IEEE PES T&D Conf. Expo.*, 2014, pp. 1–5.